

A comparison of annealing kinetics in crystalline and amorphous InP

L. Cliche, S. Roorda, G. E. Kajrys, and R. A. Masut

Citation: *J. Appl. Phys.* **79**, 2142 (1996); doi: 10.1063/1.361073

View online: <http://dx.doi.org/10.1063/1.361073>

View Table of Contents: <http://jap.aip.org/resource/1/JAPIAU/v79/i4>

Published by the [American Institute of Physics](#).

Related Articles

Analysis of optical properties of porous silicon nanostructure single and gradient-porosity layers for optical applications

J. Appl. Phys. **112**, 053506 (2012)

Post-growth surface smoothing of thin films of diindenoperylene
Appl. Phys. Lett. **101**, 033307 (2012)

Post-growth surface smoothing of thin films of diindenoperylene
APL: Org. Electron. Photonics **5**, 156 (2012)

Disorder enhancement due to structural relaxation in amorphous Ge₂Sb₂Te₅
Appl. Phys. Lett. **100**, 213506 (2012)

Analysis of vacancy-induced amorphization of single-layer graphene
Appl. Phys. Lett. **100**, 203105 (2012)

Additional information on J. Appl. Phys.

Journal Homepage: <http://jap.aip.org/>

Journal Information: http://jap.aip.org/about/about_the_journal

Top downloads: http://jap.aip.org/features/most_downloaded

Information for Authors: <http://jap.aip.org/authors>

ADVERTISEMENT



AIP Advances

Now Indexed in
Thomson Reuters
Databases

Explore AIP's open access journal:

- Rapid publication
- Article-level metrics
- Post-publication rating and commenting

A comparison of annealing kinetics in crystalline and amorphous InP

L. Cliche, S. Roorda, and G. E. Kajrys

Groupe de recherche en physique et technologie des Couches Minces, Département de Physique, Université de Montréal C.P. 6128 succ. Centre-ville, Montréal, Québec H3C 3J7, Canada

R. A. Masut

Groupe de recherche en physique et technologie des Couches Minces, Département de Génie Physique, École Polytechnique de Montréal, C.P. 6079 succ. centre-ville, Montréal, Québec H3C 3A7, Canada

(Received 21 August 1995; accepted for publication 9 November 1995)

Relaxation of ion-induced strain in crystalline InP is compared with structural relaxation of amorphous InP. Crystalline InP was bombarded with Se ions at low fluence to produce a damaged surface layer. The room temperature evolution of strain in this layer was determined by high-resolution x-ray diffraction and compared to the evolution of the defect-activated viscosity of amorphous InP during similar room temperature structural relaxation. Both processes can be described by double exponential decay functions with characteristic times of a few hours to a few days. © 1996 American Institute of Physics. [S0021-8979(96)02704-X]

Structural relaxation, an intrinsic network rearrangement accompanied by changes in vibrational, structural, and thermodynamic properties, is known to occur in all amorphous solids. In the case of *a*-Si, it has been suggested that structural relaxation is controlled by annihilation of point defects in the network.¹ Calorimetric measurements indicated that defect annihilation in *a*-Si exhibits the same kinetics and temperature dependencies as that in heavily damaged *c*-Si. Further evidence for a relationship between structural defects in *a*-Si and lattice defects in *c*-Si came from photocarrier lifetime measurements.²

The response of the structure of InP to ion bombardment is quite different from that of Si. In the low fluence regime, InP contracts,³ as opposed to most crystalline semiconductors which expand when subjected to ion bombardment. Some of the implantation damage anneals out spontaneously during room temperature storage.⁴ Amorphous InP is more dense than the crystalline phase⁵ (again, unlike most other semiconductors) and exhibits a subsequent structural relaxation which consists of a volume expansion, partly accommodated by shear plastic flow which is mediated by flow defects.⁶ In view of these differences, it is of interest to search for a similarity in the anneal kinetics of amorphous and crystalline InP. As a single probe of the defect density in both kinds of material is not available, we have compared the evolution of radiation-induced strain associated with lattice defects in *c*-InP with that of flow defects in *a*-InP.

Semi-insulating InP samples with cleaned surfaces were mounted, with a good thermal contact, on a copper block inside the implantation chamber. Two samples used for x-ray analysis were identically implanted at room temperature with 15 MeV 1×10^{13} Se/cm². The beam current was kept low in order to maintain the total power incident on the target below 0.5 W. All the samples were kept in liquid nitrogen between experiments and their age refers to the time spent out of the liquid nitrogen reservoir.

The low fluence ion-bombarded *c*-InP samples were analyzed by x-ray diffraction. We used a Phillips five-crystal x-ray diffractometer with a Cu K_{α} x-ray source. The (004) rocking curves were analyzed with the help of a computer

simulation program which was originally developed by Wie.⁷ Our version of the program can simulate x-ray rocking curves of different reflections for elemental and binary compounds and is based on dynamical x-ray diffraction theory. The program incorporates the depth profiles of the lattice strain and lattice damage caused by the ion irradiation. The decrease in the intensity of the diffracted x rays caused by lattice damage is taken into account by averaging the structure factor over a spherically symmetric Gaussian distribution of the atomic displacements. The strain and damage profiles were modeled to fit the measured diffraction spectra.

The surfaces of ion amorphized InP (*a*-InP) samples were profiled with a stylus profilometer (Dektak 3030ST). We repeated these measurements several times over a period of about 70 days following implantation. The out-of-plane deformation of the implanted samples was deduced from the *c*-InP/*a*-InP steps which were measured on the surface profiles. The in-plane deformation was deduced from the radius of curvature which was also obtained from the surface profile. We have calculated the viscosity of the material from the time evolution of the in-plane and out-of-plane deformations. A detailed description of *a*-InP sample preparation and of the calculation is given elsewhere.⁶

Figure 1 shows the evolution of the symmetric (004) x-ray diffraction spectrum of one of the two implanted InP samples which was aged at room temperature following the low fluence ion implantation. The first peak on the left-hand side of each curve corresponds to the x-ray diffraction from the undamaged lattice planes of the underlying substrate. The substrate peak was identified by overlaying the diffraction spectrum of an implanted region with one taken on an adjacent unimplanted region. The angle shown in Fig. 1 is with respect to this position. The diffracted light which appears on the right-hand side of the substrate peak comes from the damaged portion of the sample. Diffraction at higher Bragg angles indicates a compaction of the damaged lattice planes. Two peaks can be distinguished coming from the damaged region of the sample. Referring to the spectrum of the 1 h old

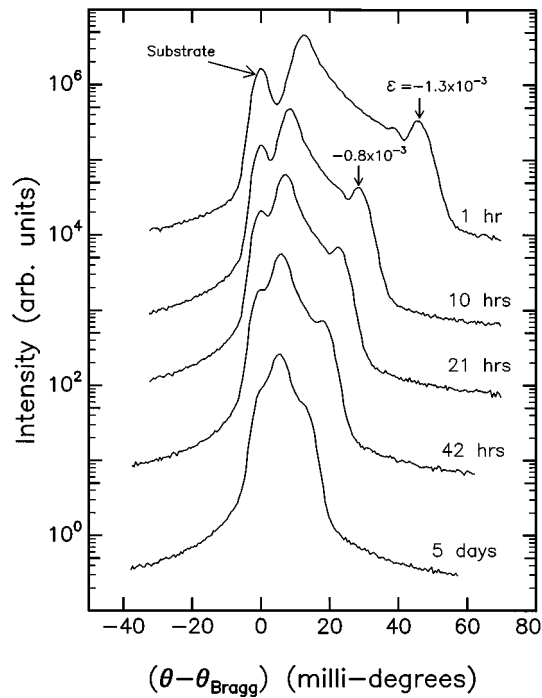


FIG. 1. X-ray diffraction spectra of InP implanted with 15 MeV, 1×10^{13} Se/cm², and aged at room temperature. Indicated is the highest perpendicular strain measured in the damage layer.

sample, we measured for this symmetric reflection a perpendicular strain of -0.035% for the middle peak and -0.13% for the right-hand peak (high strain peak). As time passes, the portion to the right-hand side of the diffraction spectrum shifts slowly toward the substrate peak. This indicates that the damaged region which was initially compacted, partly recovers its volume by means of an expansion in the out-of-plane direction. As the age of the sample increases from 1 h to 5 days, the most highly strained region of the sample (the far right-hand structure in the spectrum) decreases from -0.13% to approximately -0.04% of strain, respectively.

Figure 2(a) shows the measured spectrum (points) as well as the calculated curve (solid line) of a sample 1 h after ion implantation (the top curve from Fig. 1). Figure 2(b) shows the modeled input parameters of the calculation which are the depth profiles of the component of the lattice strain (solid line) and the atomic displacement (dashed line) normal to the surface. A comparison of simulated spectra of a variety of damage and strain profiles reveals that the strongest diffraction peak adjacent to the substrate peak is coming from a constant surface strain region extending to a depth of about $3.5 \mu\text{m}$ (see mark A). The second diffraction peak, on the far right-hand of Fig. 2(a), comes from a highly strained region centered around $5 \mu\text{m}$ (see mark B). This peak is attenuated by a relatively large incoherent scattering from point defects in this layer. In the depth profile 2(b), this shows up as a peak in "atomic displacement" near the end of the range (see mark C). This highly damaged buried region is distinct from the near-surface region where a low damage density predominates. Note: horizontal arrows with the marks A, B and C refer to peak heights, and vertical arrows to peak positions.

Strain in the implanted layer is closely related to the

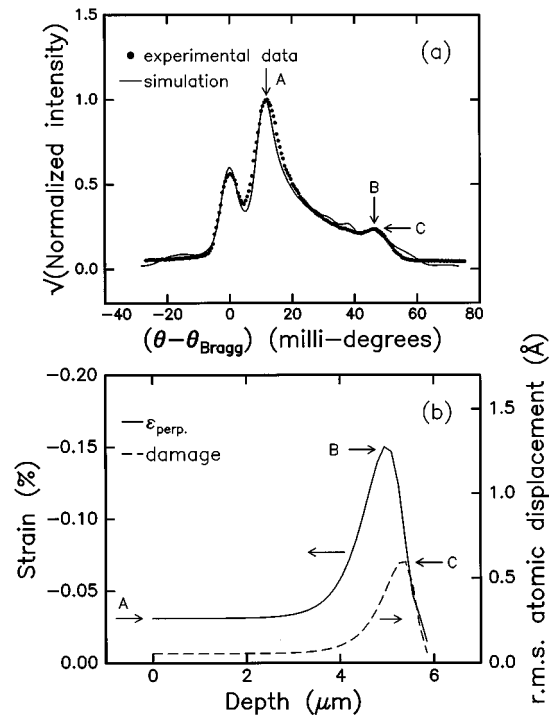


FIG. 2. (a) X-ray diffraction spectrum of an InP sample 1 h after ion implantation (points) along with the calculated curve (solid line). (b) Corresponding strain (solid line) and atomic displacement (dashed line) profiles modeled to reproduce the x-ray diffraction spectrum. The three indications A, B and C indicate corresponding features in (a) and (b).

density of damage. It is known that point defects in a material are accompanied by a strain field due to local rearrangements involving bond-angle distortions. In the case of InP, it has been observed experimentally that, for low damage densities (less than 5 at. % point defects), the strain level is roughly proportional to the density of defects.³ The evolution of the strain profile can therefore be taken to qualitatively follow the evolution of the density of damage in the implanted sample.

From the family of diffraction curves (Fig. 1), we have extracted the maximum perpendicular strain values in the damaged layer of the crystal as a function of relaxation time. This was done by measuring the peak separation between the substrate peak and the maximum strain peak (the far right-hand side of Fig. 1). We show in Figure 3 the time evolution of the strain (filled triangles) in the damaged crystal as it anneals out at room temperature. The data could be fit with a double exponential decay function (line through triangles) but not with single exponential or bimolecular decay functions. The time constants were found to be 4.3 ± 0.3 and 41 ± 3 h. These values are much shorter than those reported by Akano *et al.* who used ion channeling to characterize room temperature annealing of Si-implanted *c*-InP (shown as squares in Fig. 3).

Figure 3 also shows the indirectly determined defect evolution in *a*-InP.⁶ Recall briefly that *a*-InP first compacts during ion amorphization and then expands during room temperature structural relaxation. This expansion is accompanied by shear plastic flow which is mediated by the viscosity of the material. Plastic flow in amorphous com-

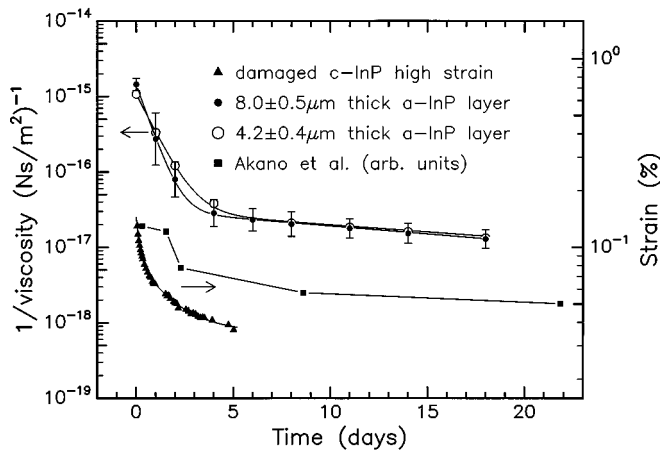


FIG. 3. Evolution of the strain (filled triangles) in damaged *c*-InP and of $1/\eta$ of two *a*-InP layers of two different thickness (filled and open circles). The solid lines are fitting results of double exponential decay functions. Also shown is the evolution of ion damage in InP, deduced from ion channeling measurements by Akano *et al.* (filled squares) (see Ref. 4).

pounds is basically described in terms of flow defects. A flow defect is a defect in the amorphous structure which, upon application of a shear stress, permits atomic rearrangements that produce macroscopic shear strain. Using an elementary theory of plastic flow, it can be demonstrated that the viscosity of the material is inversely proportional to the density of flow defects.⁸

The viscosity η of the *a*-InP sample has been measured immediately after implantation and during the following three months. In Fig. 3 we compare the strain relaxation of the damaged crystal with the time dependence of $1/\eta$ for two samples with two different thicknesses of the *a*-InP layer (the filled and open circles). The two sets of data have been fit with double exponential decay functions (the solid lines) and the average time constants were found to be 17 ± 3 h and 21 ± 3 days. Bimolecular kinetics did not give good fitting results, as was the case for the strain relaxation measurements.

The strain in *c*-InP decreases by a factor of about 4 over 5 days while during the same period, $1/\eta$ of *a*-InP decreases by a factor 60. At first, such a difference appears surprising. However, the strain measurement in *c*-InP is an indicator for the total defect density, whereas the viscosity measurement in *a*-InP monitors only the subset of defects that happens to be mobile at room temperature and is responsible for flow. Complete annealing of this subset does not mean that all of the defects in *a*-InP have been removed.

In past decades, extensive investigations have been done on amorphous Si (*a*-Si) in order to understand the properties of a structurally disordered network and the thermally induced changes of the structure also known as structural relaxation. Two different scenarios have been considered for structural relaxation in *a*-Si. In the first scenario, the network rearranges itself by an overall change in its topology. That is, every atom contributes to structural relaxation by small local changes or short-range ordering. This has no analogue in crystal Si (*c*-Si) which has long-range order. In the second scenario, structural relaxation is controlled by annihilation of

point defects, a process similar to the mechanism of radiation damage recovery in *c*-Si. In light of several recent experimental results^{1,2} indicating an intimate relation between structural relaxation in *a*-Si and defect removal in ion-damaged *c*-Si, it was proposed that structural relaxation is in fact annihilation of defects in the *a*-Si network. We can now make a similar comparison for InP, using the data shown in Fig. 3. In both cases, we see an initial fast decrease of the defect density followed by a second, slower anneal stage. The time constants are longer in *a*-InP than in *c*-InP.

Speculating about the origin of the difference in time constants, we note that there are two possible explanations. One would be that the anneal processes in *a*- and *c*-InP are intrinsically different, even though both show a qualitatively similar behavior. The other would be that it is related to the difference in initial defect level in both phases. In this context, it is recalled that the similarity in *c*-Si and *a*-Si anneal kinetics holds true only for similar, high damage levels, on the order of a few atomic percent;¹ if the damage level is decreased to a few ppm, the anneal behavior in *c*-Si changes considerably.⁹ We estimate that the defect concentration in our *a*-InP samples exceeds that in *c*-InP.

In conclusion, we have compared the structural relaxation of the amorphous and crystalline phases of ion-implanted InP. In the crystalline phase, the relaxation was probed by means of high-resolution x-ray diffraction while for the amorphous phase, we have deduced the evolution of the density of flow defects from the viscosity of the material. The relaxation profiles are well described by double exponential decay functions. For *c*-InP, the strain relaxation curve is characterized by a steep recovery with a measured time constant of 4.3 ± 0.3 h followed by a slower stage with a time constant of 41 ± 3 h. We find two stages of recovery in *a*-InP; a steep initial recovery with $\tau_1 = 17 \pm 3$ h and a slower recovery $\tau_2 = 21 \pm 3$ days. The qualitative correspondence of the recovery curves in both phases of InP is consistent with the general idea developed for Si that there is a similarity between the anneal mechanisms in ion damaged *c*-InP and *a*-InP.

The authors wish to thank C. R. Wie for permission to use his software for x-ray diffraction analysis. This work is financially supported by the Natural Science and Engineering Research Council of Canada (NSERC) and the Fonds pour la Formation de Chercheurs et l'Aide à la Recherche (FCAR).

¹S. Roorda, W. C. Sinke, J. M. Poate, D. C. Jacobson, S. Dierker, B. S. Dennis, D. J. Eaglesham, F. Spaepen, and P. Fuoss, *Phys. Rev. B* **44**, 3702 (1991).

²P. A. Stolk, F. W. Saris, A. J. M. Berntsen, W. F. van der Weg, L. T. Sealy, R. C. Barklie, G. Krötz, and G. Müller, *J. Appl. Phys.* **75**, 7266 (1994).

³C. Ascheron, A. Schindler, R. Flaggmeyer, and G. Otto, *Nucl. Instrum. Methods B* **36**, 163 (1989).

⁴U. G. Akano, I. V. Mitchell, and F. R. Shepherd, *Appl. Phys. Lett.* **59**, 2570 (1991).

⁵L. Cliche, S. Roorda, and R. Masut, *Appl. Phys. Lett.* **65**, 1754 (1994).

⁶L. Cliche, S. Roorda, and R. Masut, *Nucl. Instrum. Methods B* **96**, 319 (1995).

⁷C. R. Wie, T. A. Tombrello, and T. Vreeland, Jr., *J. Appl. Phys.* **59**, 3743 (1986).

⁸F. Spaepen, in *Physics of Defects*, edited by R. Balian *et al.* (Les Houches Lectures XXXV, North-Holland, Amsterdam, 1981), p. 154.

⁹S. Roorda, in *Materials Synthesis and Processing Using Ion Beams*, edited by R. J. Culbertson *et al.* [*Mater. Res. Soc. Symp. Proc.* **316**, 159 (1994)].